Quarkonium Production in pA Collisions

R. Vogt

Nuclear and Chemical Sciences Division, Lawrence Livermore National Laboratory, Livermore, CA 94551, USA

Physics Department, University of California, Davis, CA 95616, USA

U.S. DEPARTMENT OF ENERGY | Office of Science

Approaches Employed to Study Quarkonium Hadroproduction in p+Pb Collisions

NLO Color Evaporation Model (CEM) + various nPDFs with uncertainties (RV, Phys. Rev. C 92 (2015) 034909)

LO Color Singlet Model (CSM) + various nPDF sets (Lansberg *et al*, Eur. Phys. J. C 61 (2009) 859)

Final-state energy loss, with or without shadowing (Arleo and Peigne, JHEP 1303 (2013) 122; 1305 (2013) 155)

Color-Glass Condensate (CGC): CGC + CEM (Fujii and Wantanabe, Nucl. Phys. A 915 (2013) 1); CGC + NRQCD (Ma, Venugopalan and Zhang, Phys. Rev. D 92 (2015) 071901)

Comover approach, differentiates between J/ψ and ψ' (Ferreiro, Phys. Lett. B 749 (2015) 98)

See p+Pb predictions for 5 TeV run compared to data, arXiv:1605.09479 and references therein for more details

Start with NLO CEM and Its Uncertainties

Pinning Down J/ψ CEM Parameters by Fitting $\sigma_{c\bar{c}}$

Caveat: full NNLO cross section unknown, could still be large corrections

Employ $m = 1.27$ GeV, lattice value at $m(3\,\mathrm{GeV})$ and use subset of $c\bar{c}$ total cross section data to fix best fit values of μ_F/m and μ_R/m

Result with $\Delta\chi^2 = 1$ gives uncertainty on scale parameters

LHC results from ALICE agrees well even though not included in the fits

Same mass and scale parameters used to calculate J/ψ

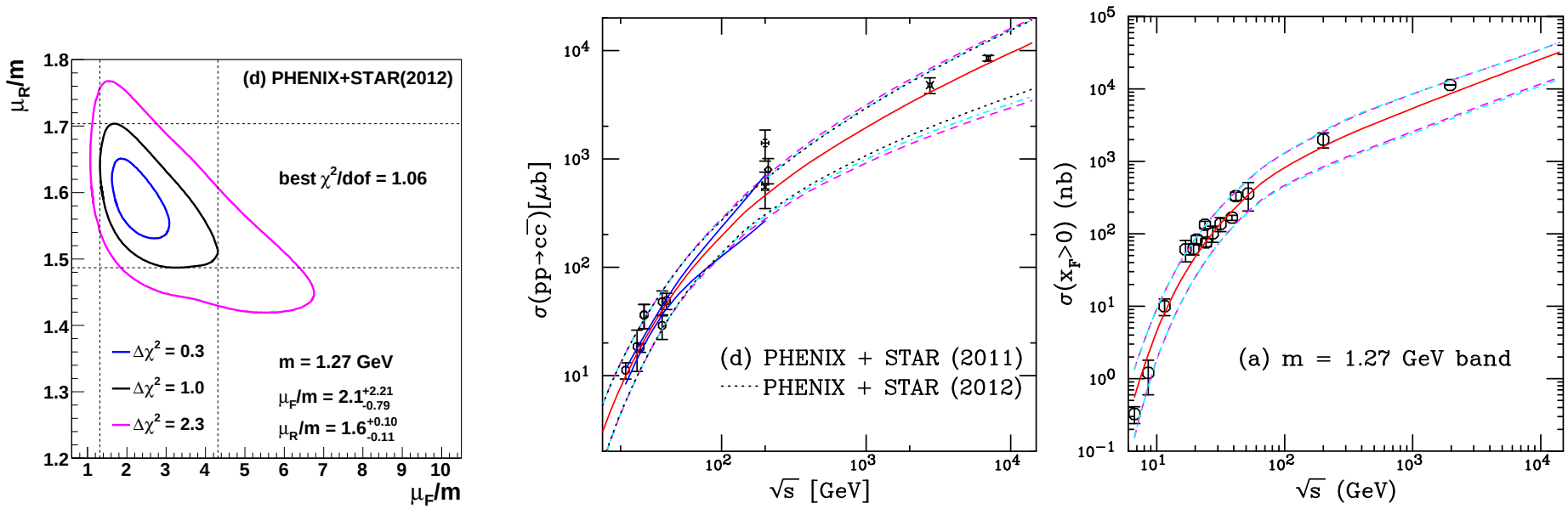

Figure 1: (Left) The χ^2/dof contours for fits employing the STAR 2011 cross section. The best fit values are given for the $\Delta\chi^2 = 1$ contours. (Center) The energy dependence of the charm total cross section compared to data. The best fit values are given for the furthest extent of the $\Delta\chi^2 = 1$ contours. The central value of the fit is given by the solid red curve while the dashed magenta curves and dot-dashed cyan curves show the extent of the corresponding uncertainty bands. The dashed curves outline the most extreme limits of the band. The dotted black curves show the uncertainty bands obtained with the 2012 STAR results while the solid blue curves in the range $19.4 \leq \sqrt{s} \leq 200$ GeV represent the uncertainty obtained from the extent of the $\Delta\chi^2 = 2.3$ contour. (Right) The uncertainty band on the forward J/ψ cross section. The dashed magenta curves and dot-dashed cyan curves show the extent of the corresponding uncertainty bands. The dashed curves outline the most extreme limits of the band. (Nelson, RV, Frawley, Phys. Rev. C **87** (2013) 014908)

Calculating Mass/Scale Uncertainties in pA

The one standard deviation uncertainties on the quark mass and scale parameters calculated using EPS09 NLO central set and CT10 parton densities

If the central, upper and lower limits of $\mu_{R,F}/m$ are denoted as C, H, and L respectively, then the seven sets corresponding to the scale uncertainty are

$$(\mu_F/m, \mu_F/m) = (C, C), (H, H), (L, L), (C, L), (L, C), (C, H), (H, C)$$

Following Cacciari, Nason and RV, he extremes of the cross sections with mass and scale are located and used to calculate the uncertainty in either total cross section or some distribution

$$\begin{aligned}
\sigma_{\rm max} &= \sigma_{\rm cent} + \sqrt{(\sigma_{\mu,\rm max} - \sigma_{\rm cent})^2 + (\sigma_{m,\rm max} - \sigma_{\rm cent})^2}\ , \\
\sigma_{\rm min} &= \sigma_{\rm cent} - \sqrt{(\sigma_{\mu,\rm min} - \sigma_{\rm cent})^2 + (\sigma_{m,\rm min} - \sigma_{\rm cent})^2}\ ,
\end{aligned}$$

Calculating Mass and Scale Uncertainties on $R_{p\mathrm{Pb}}$

The mass and scale uncertainties on the ratios are calculated in 3 ways:

The first two follow Cacciari, Nason and RV shown on the previous slide

$m/\mu_F/\mu_R$ **v1 We take the ratios of p+Pb to pp for each mass and scale combination and then locate the extrema in each case – this gives the uncertainty on $R_{p\mathrm{Pb}}$ of each set, can appear odd if ratios are not very different but the extrema changes between sets (as it does for $R_{p\mathrm{Pb}}(y)$)**

$m/\mu_F/\mu_R$ **v2 We locate the mass and scale extrema and calculate the uncertainty as above and then form $R_{p\mathrm{Pb}}$ by dividing by the pp cross section calculated with the central parameter set – this forms global $R_{p\mathrm{Pb}}$ based on the cross sections rather than the shadowing ratios and is thus significantly larger, especially at low p_T, becoming smaller at high p_T (Does not apply to R_{FB})**

$m/\mu_F/\mu_R$ **v3 We add the mass and scale uncertainties in quadrature, a la EPS09, and then form $R_{p\mathrm{Pb}}$ by dividing by the central pp cross section – since this is a cumulative uncertainty rather than based on the greatest excursion from the mean, it is the largest uncertainty at low p_T. This was calculated assuming that the appropriate μ_F/m and μ_R/m pairs are $[(H,H),(L,L)]$, $[(H,C),(L,C)]$ and $[(C,H),(C,L)]$, other choices could lead to different results**

Mass and Scale Uncertainty on J/ψ $d\sigma/dp_T$

Mass and scale uncertainty bands give good agreement with p+Pb data for $p_T > 2$ GeV in all rapidity regions, best agreement with central result for $p_T > 5$ GeV

Improvement at low p_T possible by varying intrinsic k_T kick

J/ψ uncertainty due EPS09 NLO nPDF sets also shown

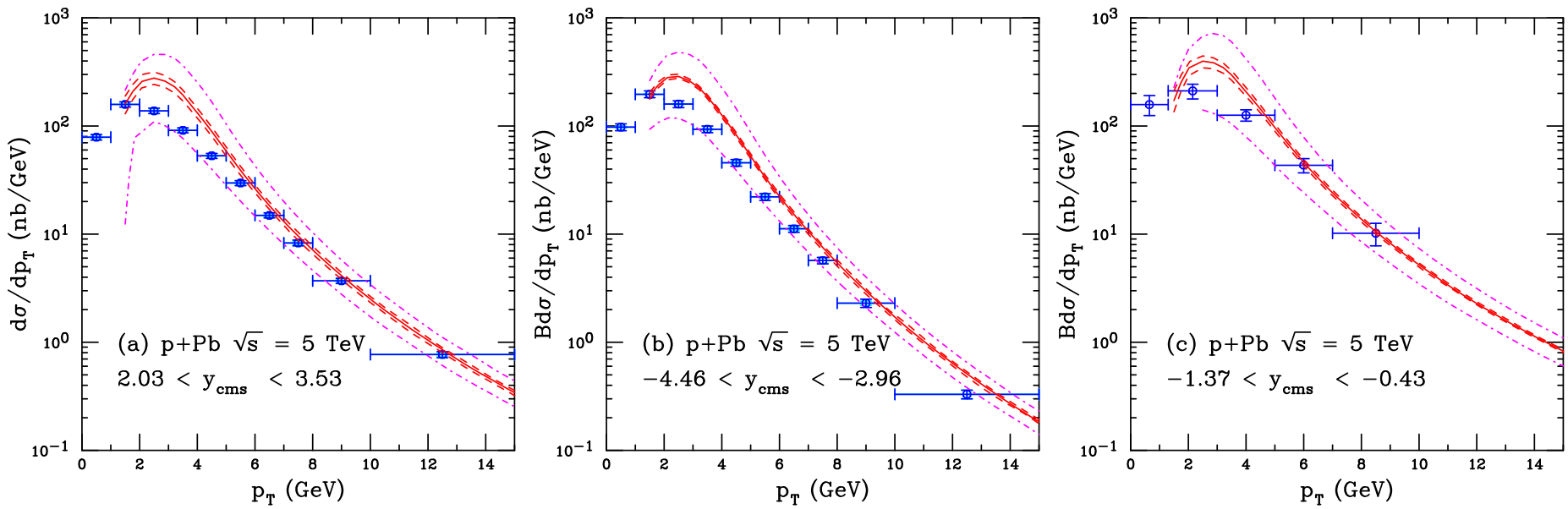

Figure 2: **The ALICE J/ψ p_T distributions at forward (a), backward (b) and midrapidity (c) at NLO in the CEM. The solid red curve is the EPS09 NLO central value while the dashed red curves are the EPS09 NLO uncertainties and the dot-dashed magenta curves are the mass and scale uncertainties.**

Mass and Scale Uncertainty Bands: $R_{p\mathrm{Pb}}(p_T)$

Uncertainties based on the differences due to EPS09 NLO alone, *i.e.* taking the extrema based on the ratios, gives very small uncertainty, smaller than EPS09 NLO

Uncertainties based on cross sections are much larger with v3 bigger than v2 at low p_T, expected since ratio is cumulative

Ratios decrease at high p_T where the scale choices are less important since $p_T \gg m$

Υ uncertainties narrower than J/ψ

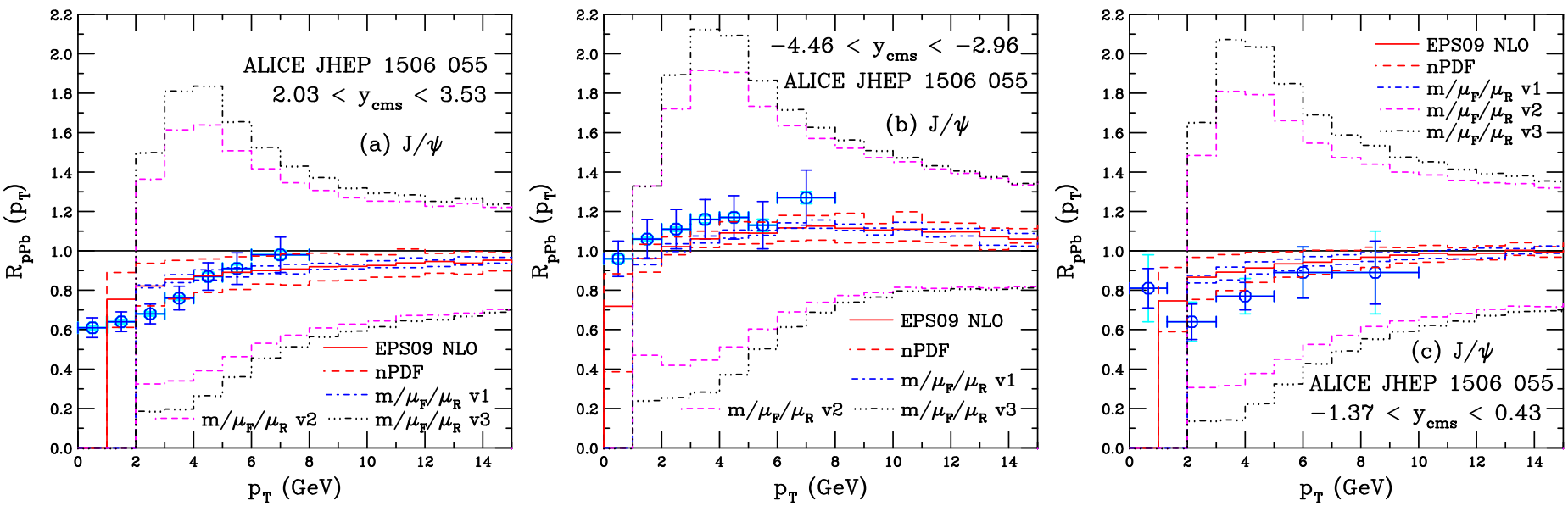

Figure 3: **The mass and scale uncertainties in the ratio $R_{p\mathrm{Pb}}(p_T)$ are compared to those for EPS09 NLO alone for ALICE at forward (left), backward (middle) and mid- (right) rapidity. The EPS09 uncertainty band is shown in red while the uncertainties calculated with method v1 in blue, v2 in magenta and v3 in black.**

Next, CEM Uncertainties from Nuclear PDFs

Calculating nPDF Uncertainties in pA

EPS09 LO and EPS09 NLO based on CTEQ61L and CTEQ6M respectively, 1 central set and 30 error sets (15 parameters)

FGS (CTEQ6M) and nDS (GRV98) available at LO and NLO, EKS98 available at LO only but no uncertainties

DSSZ NLO (MSTW2008) has 1 + 50 sets; nCTEQ15/nCTEQ15np NLO (CTEQ6M) has 1 + 32 sets

Uncertainties due to shadowing:

- **EPS09 NLO upper and lower uncertainties in any observable $\mathcal{O}$ computed using the prescription**

$$(\Delta\mathcal{O}^+)^2 \approx \sum_k \left[\max\left\{\mathcal{O}(S_k^+) - \mathcal{O}(S^0), \mathcal{O}(S_k^-) - \mathcal{O}(S^0), 0\right\}\right]^2$$
$$(\Delta\mathcal{O}^-)^2 \approx \sum_k \left[\max\left\{\mathcal{O}(S^0) - \mathcal{O}(S_k^+), \mathcal{O}(S^0) - \mathcal{O}(S_k^-), 0\right\}\right]^2$$

  The uncertainties are thus not necessarily symmetric, $\mathcal{O}^+ = \mathcal{O}_{\text{cent}} + \Delta\mathcal{O}^+$, $\mathcal{O}^- = \mathcal{O}_{\text{cent}} - \Delta\mathcal{O}^-$,

- **DSSZ and nCTEQ uncertainty calculated by differences between the results with the upper and lower limits on a parameter are symmetric and added in quadrature, $\mathcal{O} = \mathcal{O}_{\text{cent}} \pm \Delta\mathcal{O}$**

$$\Delta\mathcal{O} = \frac{1}{2}\left[\sum_{i=1}^{N_{\text{param}}} [\mathcal{O}(S_i^+) - \mathcal{O}(S_i^-)]^2\right]^{1/2}$$

NLO vs LO

The nPDF set should be appropriate to the order of the calculation – however, using EPS09 NLO in both LO and NLO CEM calculations agrees better than consistent EPS09 LO in LO and EPS09 in NLO results

Inconsistency between LO and NLO EPS09 CEM results is due to the differences between CTEQ61L and CTEQ6M: at low x CTEQ61L is fairly flat at Q_0^2 while CTEQ6M is valence-like

For nDS and nDSg, LO and NLO agree well, small differences due to x and scale, not between GRV98LO and GRV98NLO
For NLO-only nPDFs, LO can be a proxy for NLO (not EPS09 though)

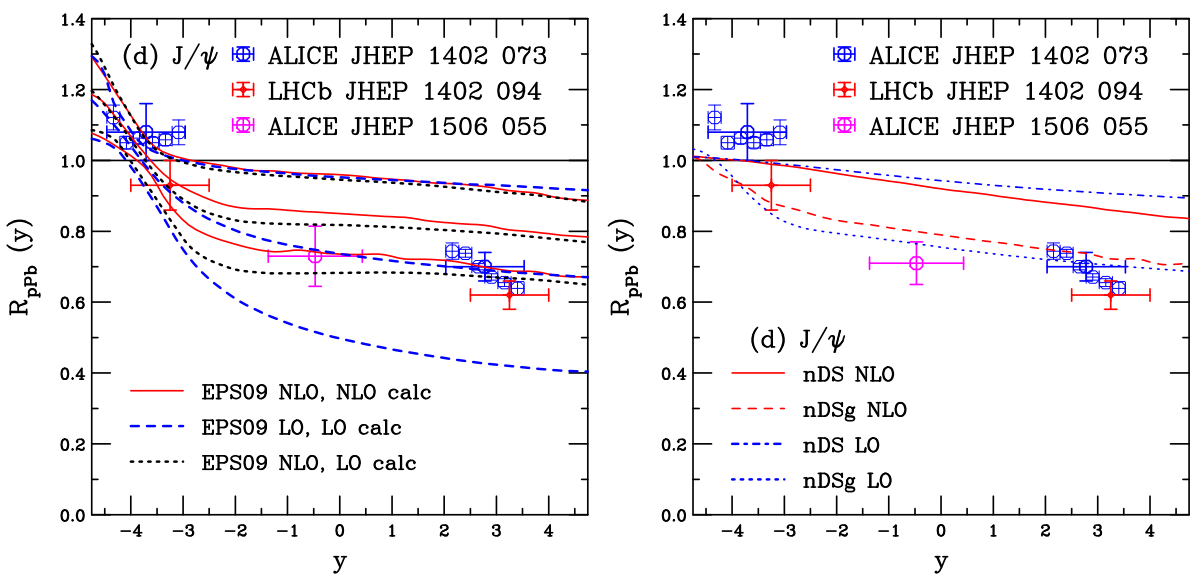

Figure 4: **(Left) The EPS09 LO in the LO CEM (blue), EPS09 NLO in the NLO CEM (red), and EPS09 NLO in the LO CEM (black) J/ψ uncertainty bands for $R_{p\mathrm{Pb}}(y)$ at $\sqrt{s_{NN}} = 5$ TeV. (Right) The same results for nDS and nDSg results at LO (blue) and NLO (red) for J/ψ production.**

Comparison of Results with Different nPDF Sets: J/ψ

Of the older sets, EKS98 (LO only) agrees best with the data

DSSZ sets have too little gluon shadowing to agree with forward rapidity results

central nCTEQ15(np) stronger shadowing than data but uncertainty bands are broad, especially the np sets which don't include the RHIC inclusive π^0 data and so are less constrained

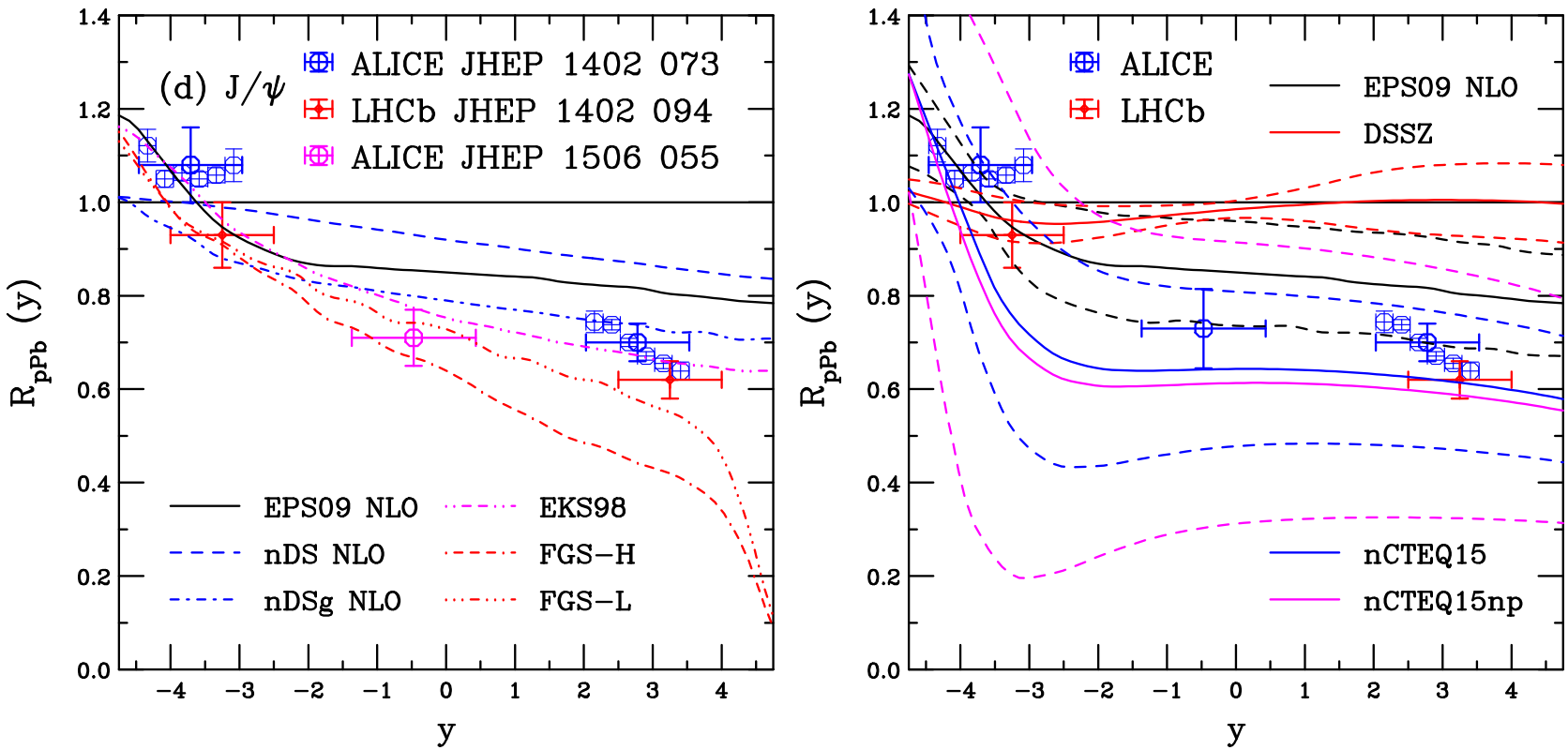

Figure 5: **(Left) Comparison of central EPS09 NLO (JHEP 0904 (2009) 065) with NLO CEM calculations with EKS98 (Eur. Phys. J. C 9 (1999) 61), FGS-H, FGS-L (Phys. Rept. 512 (2012) 255), nDS and nDSg (Phys. Rev. D 69 (2004) 074028). (Right) Sets with uncertainties are compared. The EPS09 NLO uncertainty band is shown with NLO bands calculated with a proxy LO calculation for DSSZ (Phys.Rev. D 85 (2012) 074028), nCTEQ15 and nCTEQ15np (Phys. Rev. D 93 (2016) 085037).**

Comparison of Results with Different nPDF Sets: Υ

LHCb and ALICE data do not agree well with each other (if generous, there is barely 1σ agreement) – more data needed to resolve differences

Calculations all suggest some degree of antishadowing at backward rapidity and reduced shadowing at forward rapidity relative to J/ψ, due to larger scale and large x, more consistent with LHCb data

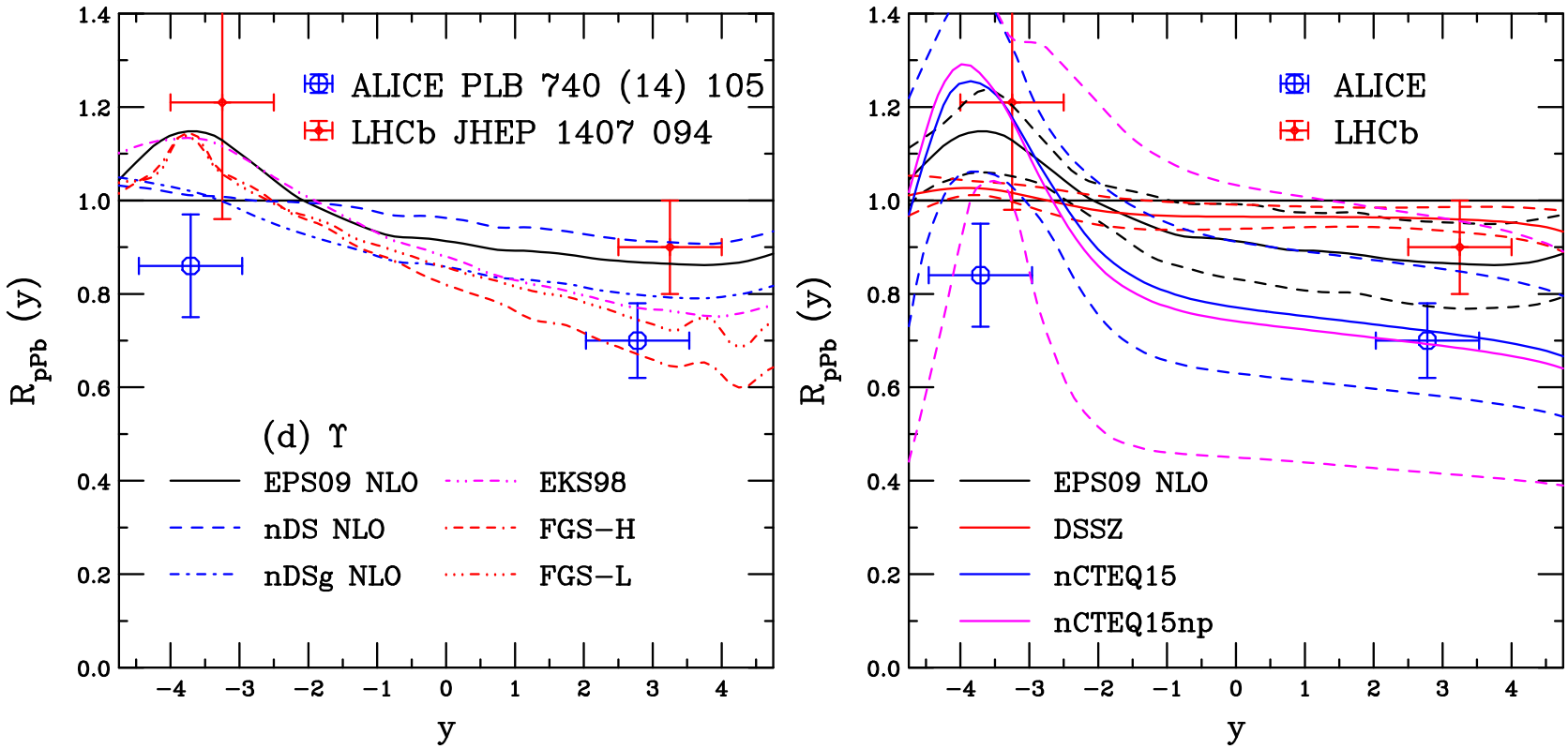

Figure 6: **(Left) Comparison of central EPS09 NLO with NLO CEM calculations with EKS98, FGS-H, FGS-L, nDS and nDSg. (Right) Sets with uncertainties are compared. The EPS09 NLO uncertainty band is shown with NLO bands calculated with a proxy LO calculation for DSSZ, nCTEQ15 and nCTEQ15np.**

Other Approaches to Cold Matter Quarkonium Suppression

LO CSM Calculation with LO nPDFs (Lansberg *et al*)

LO color singlet model (CSM) to calculate production at low p_T

They make the point that theirs is a $2 \longrightarrow 2$ kinematics ($gg \to J/\psi g$) relative to $2 \longrightarrow 1$ kinematics of LO CEM (NLO CEM is $2 \longrightarrow 3$ kinematics)

They use a Glauber Monte Carlo code, JIN, to calculate the appropriate $2 \longrightarrow 2$ kinematics, sampling the x and Q^2 for the shadowing function, doesn't actually seem to be matrix elements involved in JIN

$\mu_F = (0.75, 1, 2)\sqrt{M^2 + p_T^2}$**, no μ_R scale specified**

Using LO CSM modifies R_{pA} relative to LO CEM due to shadowing because LO CEM has $p_T = 0$ for the J/ψ ($2 \longrightarrow 1$ kinematics, thus y dependence only), other differences include mass and scale values used

Uncertainties in the shadowing result shown are from two particular EPS09 sets that give the minimum and maximum magnitudes of gluon shadowing, not from taking all sets in quadrature

Differences between LO CSM and LO CSM seen only at backward rapidity and can be attributed to mass and scale choice in the two calculations

Final-State Energy Loss (Arleo and Peigne)

Arleo and Peigne fit an energy loss parameter that also depends on L_A to E866 data and uses the same parameter for other energies

$$\frac{1}{A}\frac{d\sigma_{pA}(x_F)}{dx_F} = \int_0^{E_p-E} d\epsilon P(\epsilon)\frac{d\sigma_{pp}(x_F+\delta x_F(\epsilon))}{dx_F}$$

There is no production model, only a power-law parameterization of the pp cross section

$$\frac{d\sigma_{pp}}{dp_T dx} = \frac{(1-x)^n}{x}\left(\frac{p_0^2}{(p_0^2+p_T^2)}\right)^m$$

Parameters n and m are fit to pp data, $n \sim 5$ at $\sqrt{s} = 38.8$ GeV, 34 at 2.76 TeV

Including shadowing as well as energy loss modifies the energy loss parameter, no significant difference in shape of fit at fixed-target energy but significant difference at higher $\sqrt{s}$

Backward x_F/y effect is large for this scenario, fails when y shift, δy, due to energy loss is comparable to y, causing enhancement at backward rapidity due to energy conservation

If the quarkonium state is produced at sufficiently backward y, where the state could hadronize within the nucleus and break up, the enhancement at $-y$ could be mitigated by absorption

Final State Energy Loss Predictions

Uncertainties shown are due to uncertainties on energy loss parameter $\hat{q} = 0.075^{+0.015}_{-0.005}$ GeV^2/fm (fixed at $\sqrt{s} = 38.8$ GeV and assumed energy independent) and the power n for the J/ψ and Υ production as a function of rapidity (strong $\sqrt{s}$ dependence)

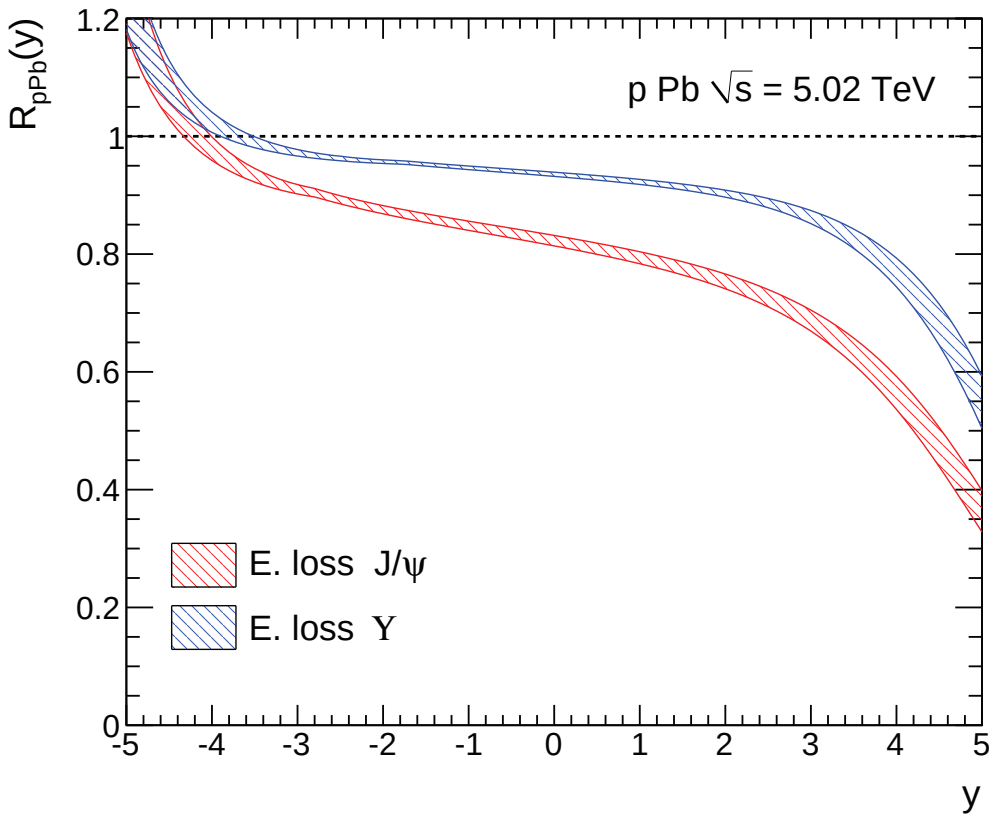

Figure 7: **The J/ψ and Υ suppression factor as a function of rapidity in p+Pb collisions at $\sqrt{s} = 5.02$ TeV for cold matter energy loss alone.**

CGC + CEM Calculations (Fujii & Watanabe)

Color Glass Condensate (CGC) calculations of gluon saturation at low momentum fraction, x, and scale $p_T << Q^2_{\rm sat}$ by Fujii *et al.* are made only in the forward direction where x_2 (in Pb nucleus) is small

Calculations done in the context of CEM

CTEQ61LO PDF used for gluon distribution on the proton side with scales between $2m_T$ and $m_T/2$, $m_T = \sqrt{M^2 + p_T^2}$ where M is the mass of the quarkonium state

Uncertainty comes from varying the saturation scale, $Q^2_{0{\rm sat},A} \sim (4-6)Q^2_{0{\rm sat},p}$, $Q^2_{0{\rm sat},p} \approx 0.16$ GeV^2 for $\gamma = 1.118$ and 0.2 GeV^2 for $\gamma = 1$ with the initial condition from the rcBK equation

$$S_Y(\vec{r}_T) = \exp\Big[-\frac{(r^2 Q^2_{0{\rm sat},p})^\gamma}{4}\ln\Big(\frac{1}{\Lambda r} + \epsilon\Big)\Big]$$

and the quark masses, $1.2 < m_c < 1.5$ GeV and $4.5 < m_b < 4.8$ GeV

CGC + NRQCD Calculations (Ma *et al.*)

The NLO NRQCD results for high p_T match onto CGC results with the same values of the nonperturbative matrix elements

For p+Pb, the saturation scale is larger, giving the p_T and y dependence of $R_{p\mathrm{Pb}}$

Nuclear suppression factors are calculated separately for each state, ratios not weighted for fraction of contribution to total, all data shown are within CGC range ($p_T < 8$ GeV)

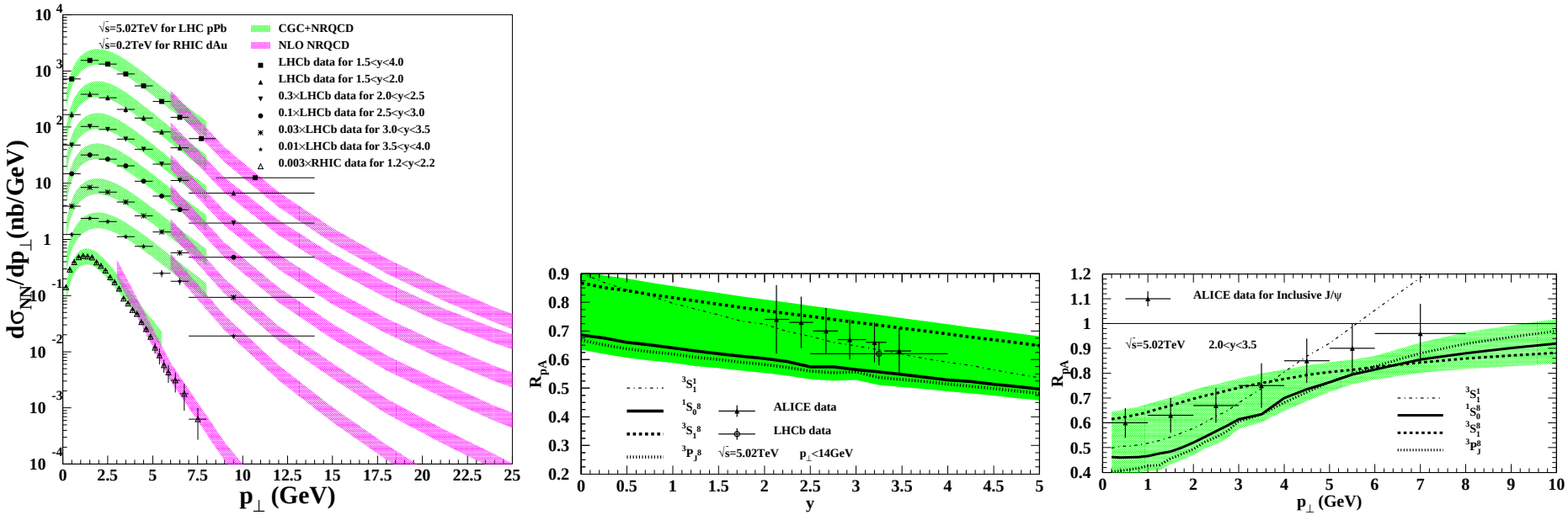

Figure 8: **(Left)** J/ψ p_T **distributions in p+Pb collisions at the LHC. (Center) Nuclear suppression factor as a function of y at forward rapidity. (Right) Nuclear suppression factor as a function of p_T in the forward rapidity region.**

Model Predictions: $R_{p\mathrm{Pb}}(y)$ for J/ψ

NLO shadowing does not describe curvature of data, LO band is larger due to greater uncertainty of EPS09 LO (only min/max used in Lansberg calculation)

Energy loss with shadowing (not shown) overestimates effect at forward rapidity

CGC + CEM (Fujii) below data, CGC + NRQCD (not shown) may agree better

EPS09 NLO and LO differ due to low x behavior of CTEQ6M and CTEQ61L

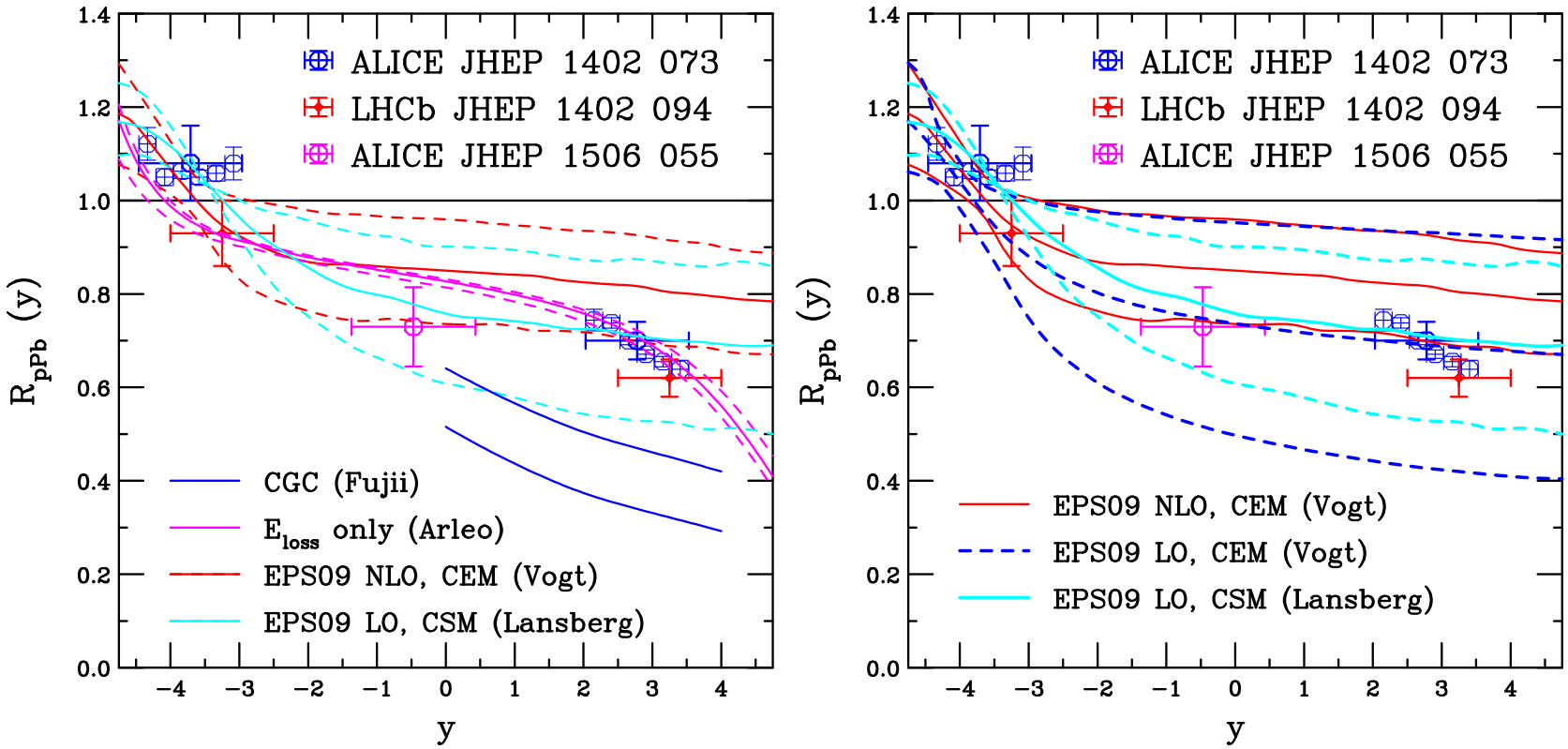

Figure 9: **(Left) The $R_{p\mathrm{Pb}}$ ratio for J/ψ as a function of y. The dashed red histogram shows the EPS09 NLO CEM uncertainties. The EPS09 LO CSM calculation by Lansberg *et al.* is shown in cyan. The energy loss calculation of Arleo and Peigne is shown in magenta. The upper and lower limits of the CGC calculation by Fujii *et al* are in blue at forward rapidity. (Right) The EPS09 LO calculations in the CEM (blue) and CSM (cyan) are compared. The CEM calculation includes the full EPS09 uncertainty added in quadrature while the CSM calculation includes only the minimum and maximum uncertainty sets. The EPS09 NLO CEM result is in red. The ALICE and LHCb data are also shown.**

Model Predictions: $R_{FB}(y)$ and $R_{FB}(p_T)$ for J/ψ

Forward ($+y$) to backward ($-y$) ratio preferable because no pp normalization required for data

Data are flatter in y than the calculations

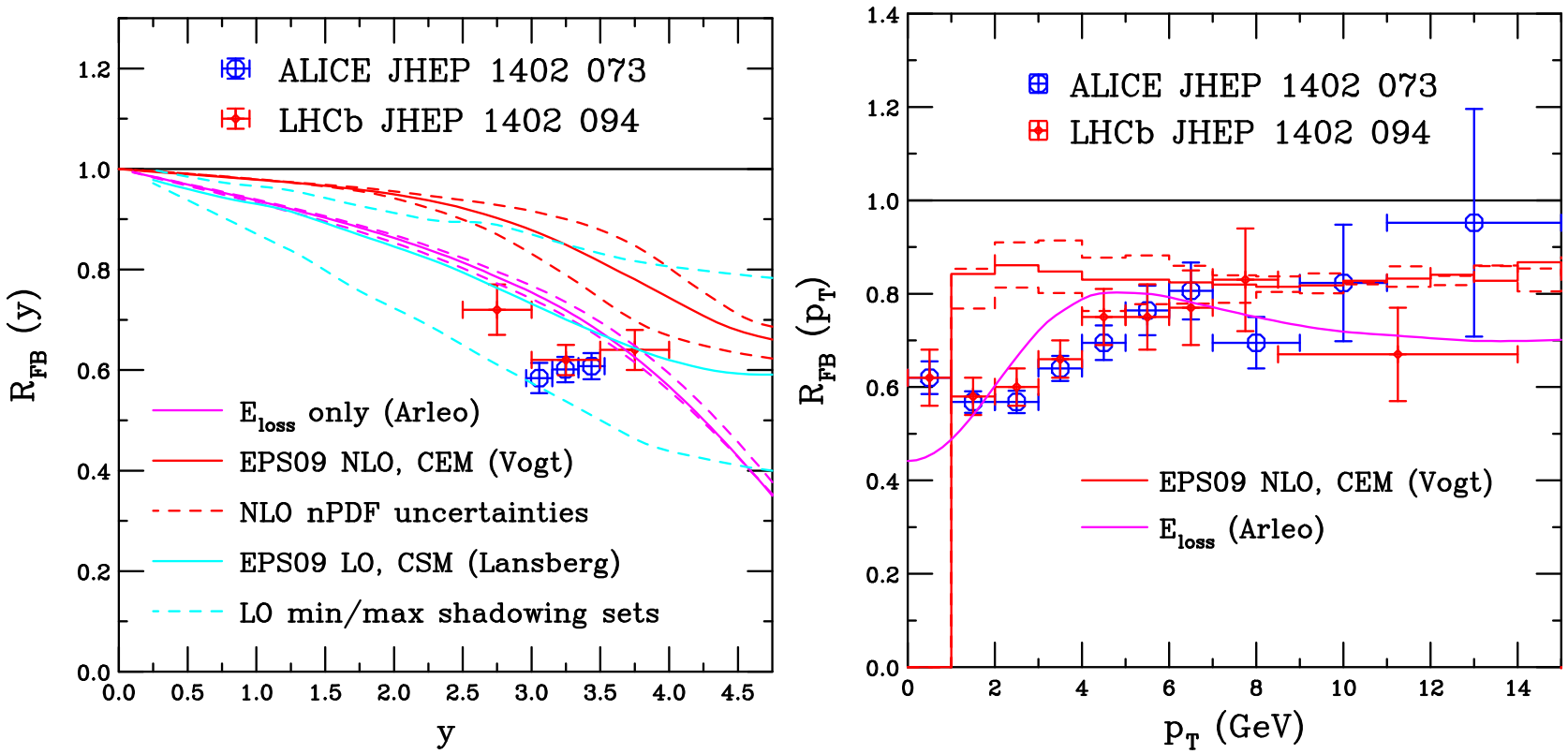

Figure 10: **The forward-backward ratio $R_{F/B}$ is shown for J/ψ as a function of y (left) and p_T (right). The dashed red histogram shows the EPS09 NLO CEM uncertainties. The energy loss only calculations of Arleo and Peigne is shown in magenta. The ALICE and LHCb data are also shown.**

Comover Calculations for J/ψ and ψ' (Ferreiro)

Difference between J/ψ and ψ' production in the comover interaction model

No nucleon absorption; EPS09 LO shadowing assumed identical for J/ψ and ψ'

The comover interaction cross section is larger for ψ', closer to $D\overline{D}$ threshold, large meson, easier to disrupt

Same comover cross sections as at lower energies, comover breakup more probable at backward rapidity where the quarkonium states have lower velocities

$$R^{\psi}_{pA}(b) = \frac{\int \mathbf{d}^2 s\, \sigma_{pA}(b)\, n(b,s)\, S^{sh}_{\psi}(b,s)\, S^{co}_{\psi}(b,s)}{\int \mathbf{d}^2 s\, \sigma_{pA}(b)\, n(b,s)}$$

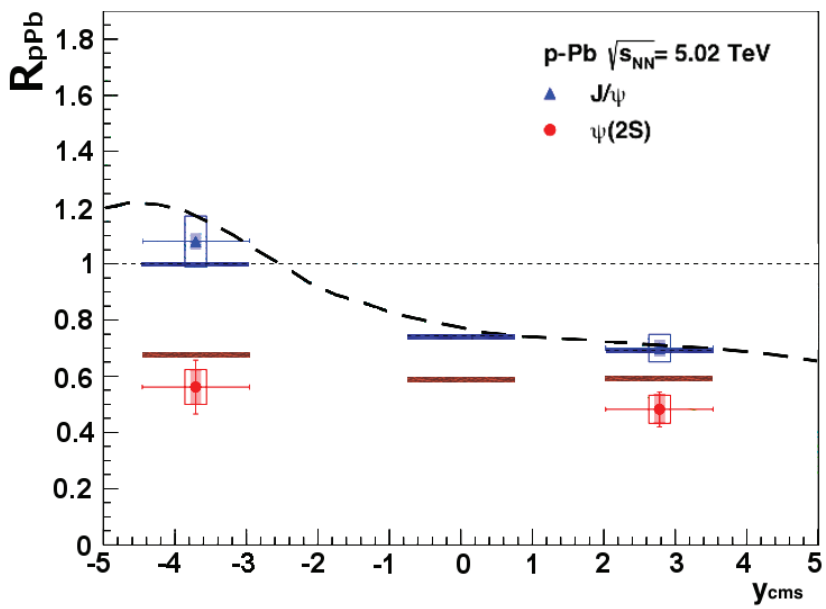

Figure 11: **The J/ψ (blue lines) and $\psi(2S)$ (red lines) nuclear modification factor R_{pPb} as a function of rapidity compared to the ALICE data (JHEP 1412 (2014) 073). The suppression due to shadowing alone (dashed line) is also shown. The ALICE results are given by the points.**

Model Predictions: $R_{p\mathrm{Pb}}(y)$ and $R_{F/B}(y)$ for Υ

Shadowing reduced in all cases for the Υ due to the larger mass scale

Interestingly, the CGC result still gives relatively large suppression at this high scale, presumably $m_b > Q_{0\mathrm{sat},A}$?

Significant difference between ALICE and LHCb data

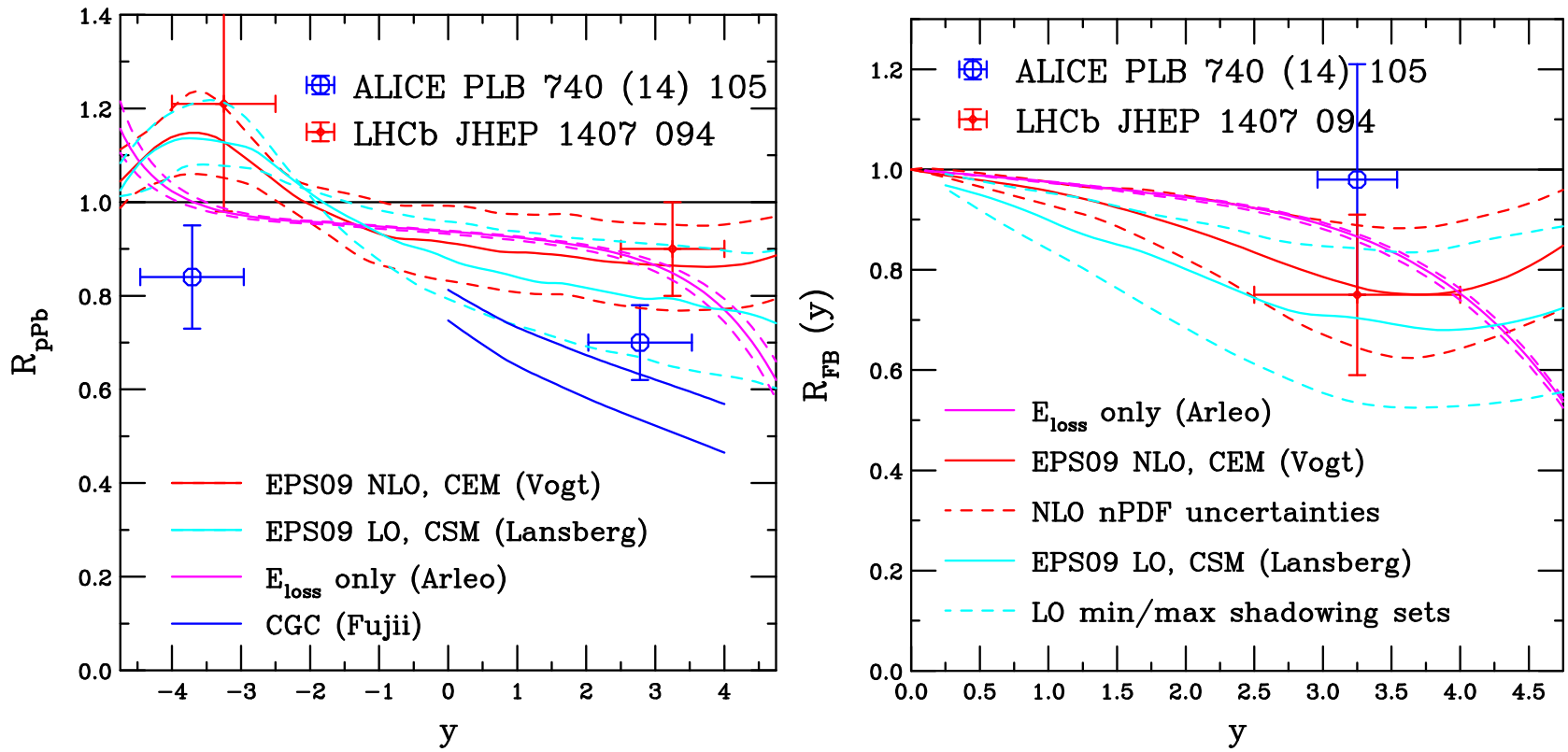

Figure 12: **(Left) The $R_{p\mathrm{Pb}}$ ratio for Υ as a function of y. The dashed red histogram shows the EPS09 NLO CEM uncertainties. The EPS09 LO CSM calculation by Lansberg *et al.* is shown in cyan. The energy loss calculation of Arleo and Peigne is shown in magenta. The upper and lower limits of the CGC calculation by Fujii *et al* are in blue at forward rapidity. (Right) The forward-backward ratio for Υ production as a function of rapidity. The same calculations are shown here except that there is no CGC result in the backward region. The ALICE and LHCb data are also shown.**

Summary

- **Differences in nPDF predictions illustrates the fact that gluon nPDF is still not very well constrained**
- **New global analyses taking the LHC p+Pb hadroproduction data into account should be done, many caveats on medium effects (energy loss vs. shadowing, saturation vs. collinear factorization)**